ELECTRODYNAMIC TETHER SATELLITE DYNAMICS MODELLING

by

KAIWEN CHEN

A Thesis Submitted to
The Hong Kong University of Science and Technology
in Partial Fulfillment of the Requirements for
the Degree of Master of Science
in Aeronautical Engineering

May 2018, Hong Kong

Authorization

I hereby declare that I am the sole author of the thesis.

I authorize the Hong Kong University of Science and Technology to lend this thesis to other institutions or individuals for the purpose of scholarly research.

I further authorize the Hong Kong University of Science and Technology to reproduce the thesis by photocopying or by other means, in total or in part, at the request of other institutions or individuals for the purpose of scholarly research.

KAIWEN CHEN

ELECTRODYNAMIC TETHER SATELLITE DYNAMICS MODELLING

by

KAIWEN CHEN

This is to certify that I have examined the above M.Sc. thesis

and have found that it is complete and satisfactory in all respects,

and that any and all revisions required by

the thesis examination committee have been made.

Prof. Xun HUANG, Thesis Supervisor

Department of Mechanical and Aerospace Engineering

29 May 2018

ACKNOWLEDGMENTS

I would never have completed this work without the help from many people. First of all, I thank my advisor, Professor Xun Huang, for his kind mentoring, helpful advices, and encouragement. I have got generous material support, well-condition laboratory experiences and engineering-oriented practice.

I thank the members of my thesis committee, Professor Xin Zhang for his insightful comments on improving this work.

I thank my colleagues in HKUST – Huanxian Bu, Zheng Liu, Wei Feng, Jiafeng Wu, Jingwen Guo, Jiaqi Song and many others. We have finished several deadlines and projects as a team. In daily life, we have been good friends and enjoy many activities in school campus. Without them, my graduate study in HKUST would not be so colorful.

I give my special thanks to Dr.Pok Wang KWAN who spent nearly a whole year instructing me on how to do research. He gave the project a lot of remarkable ideas using his sufficient engineering background and rich industry experience. When everything goes more and more complicated, his clear mind and intuition always work quite well. I learned how to proceed an engineering research project and how to analyse problems logically and incrementally from his face to face teaching.

I thank my parents for their support and encouragement.

Hope this thesis will not be the end of my academia, I hope the first half sentence is not just a hope.

TABLE OF CONTENTS

LIST OF FIGURES

LIST OF TABLES

ELECTRODYNAMIC TETHER SATELLITE DYNAMICS MODELLING

by

KAIWEN CHEN

Department of Mechanical and Aerospace Engineering

The Hong Kong University of Science and Technology

ABSTRACT

Abstract

CHAPTER 1

MOTIVATION

Satellites in orbit around Earth are used in many areas and disciplines, including space science, Earth observation, meteorology, climate research, telecommunication, navigation and human space exploration. They offer a unique resource for collecting scientific data, commercial opportunities and various essential applications and services, which lead to unrivalled possibilities for research and exploitation.

However, in the past decades, with increasing space activities, a new and unexpected hazard has started to emerge: space debris.

The Figure 1.1 showes the debris changing trend over nearly 60 years. The y direction shows the number of objects. Each point represents the monthly numberof objects in Earth Orbit. The x direction is time axis. Space debris is divided into four types, each type has its own color:

1. Fragmentation Debris
2. Spacecraft
3. Mission-related Debris
4. Rocket Bodies

The orbris increasing of Spacecraft and Rocket Bodies are quite linearly. Mission-related Debris is quite stable. The most dramatic changing type is Fragmentation Drbis and this type of debris is directly related to satellite explosion and artificial celestial body collision.

From another statistical result [], we can see this trend much more clearly. In almost 60 years of space activities, more than 5250 launches have resulted in some 42 000 tracked objects in orbit, of which about 23000 remain in space and are regularly tracked by the

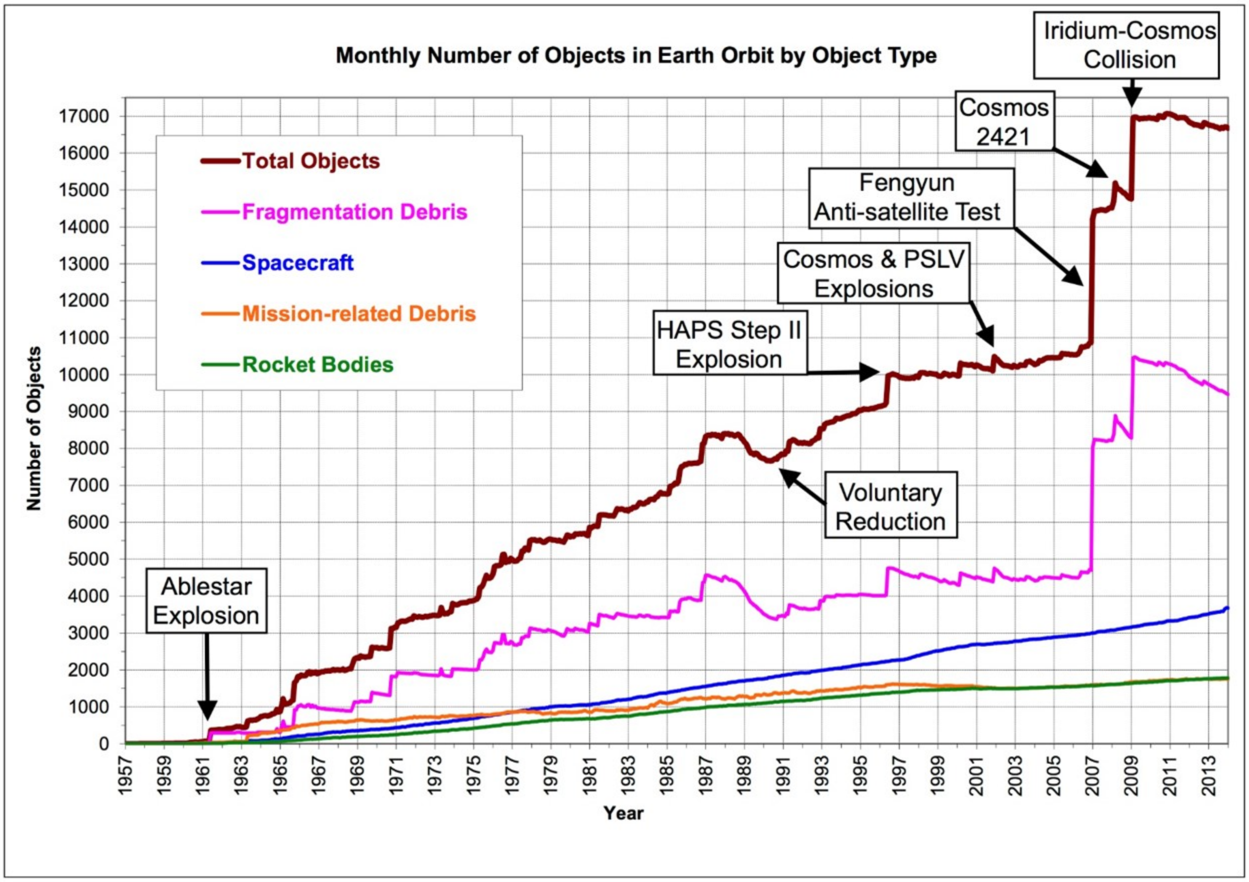

Figure 1.1. Catalogued space debris over time
[3]

US Space Surveillance Network and maintained in their catalogue, which covers objects larger than about 5âĂŞ10 cm in low-Earth orbit (LEO) and 30 cm to 1 m at geostationary (GEO) altitudes. Only a small fraction âĂŞ about 1200 âĂŞ are intact, operational satellites today.

This large amount of space hardware has a total mass of more than 7500 tonnes.

1. Spent upper stages

   About 24% of the catalogued objects are satellites (less than a third of which are operational), and about 18% are spent upper stages and mission related objects such as launch adapters and lens covers.

   More than 290 inorbit fragmentation events have been recorded since 1961. Only a few were collisions and the majority of the events were explosions of spacecraft and upper stages.

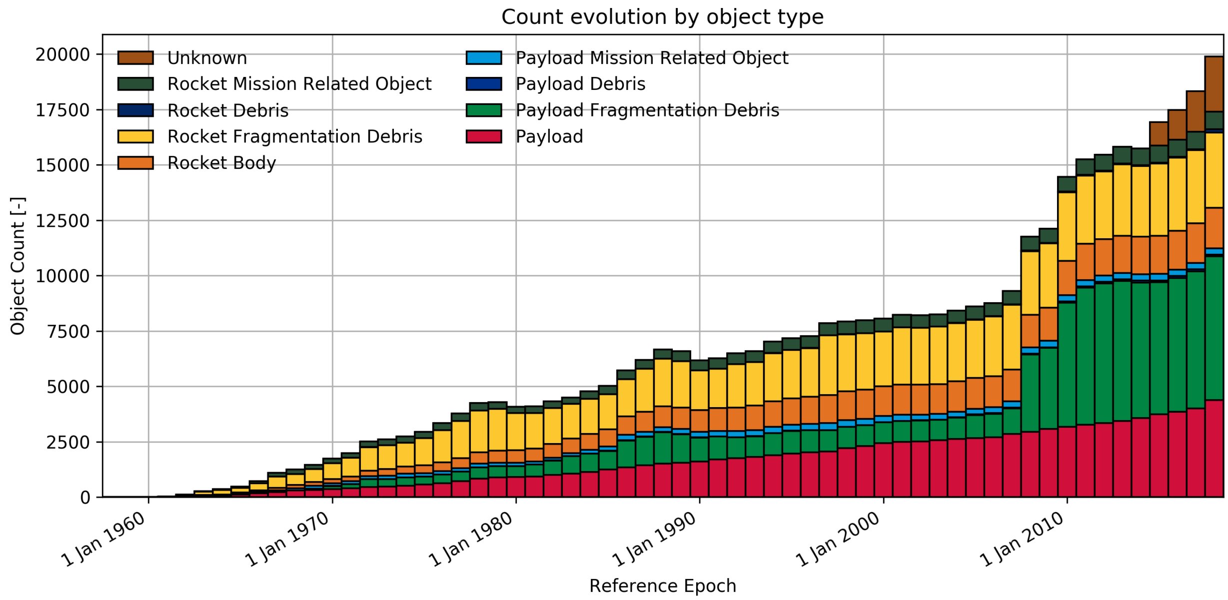

Figure 1.2. Conut evolution by object type

2. Explosions of satellites and rocket bodies

   These fragmentation events are assumed to have generated a population of objects larger than 1 cm numbering on the order of 750000. The sporadic flux from naturally occurring meteoroids may only prevail over that from human-made debris objects near sizes of 0.1-1 mm.

   The main cause of inorbit explosions is related to residual fuel that remains in tanks or fuel lines, or other remaining energy sources, that remain on board once a rocket stage or satellite has been discarded in Earth orbit.

   Over time, the harsh space environment can reduce the mechanical integrity of external and internal parts, leading to leaks and/or mixing of fuel components, which could trigger self-ignition. The resulting explosion can destroy the object and spread its mass across numerous fragments with a wide spectrum of masses and imparted velocities.

3. Antisagellite test

   Besides such accidental break-ups, satellite interceptions by surface-launched missiles have been a major contributor in the recent past.

   The Chinese FengYun-1C engagement in January 2007 alone increased the trackable space object population by 25%.

4. Other sources

   Solid rocket-motor firings, the ejection of reactor cores from Buk reactors after the end of operation of Russian radar ocean reconnaissance satellites in the 1980s and the relase of thin copper wires as part of a radio communication experiment during the Midas missions in the 1960s are the three most important sources.

The nightmare scenario that space debris experts contemplate is called the Kessler syndrome, after American astrophysicist Donald Kessler. In 1978, while working for NASA, he published an analysis[2] that showed frequent collisions exponentially increased the amount of space debris, leading to many more collisions, leading to much more debris until we lose the use of certain orbits because anything we put there would certainly be hit.

> *"Since 2002, The growth has entered into the more feared exponential trend."*

There can be absolutely no doubt that the time to do something about space debris has arrived.

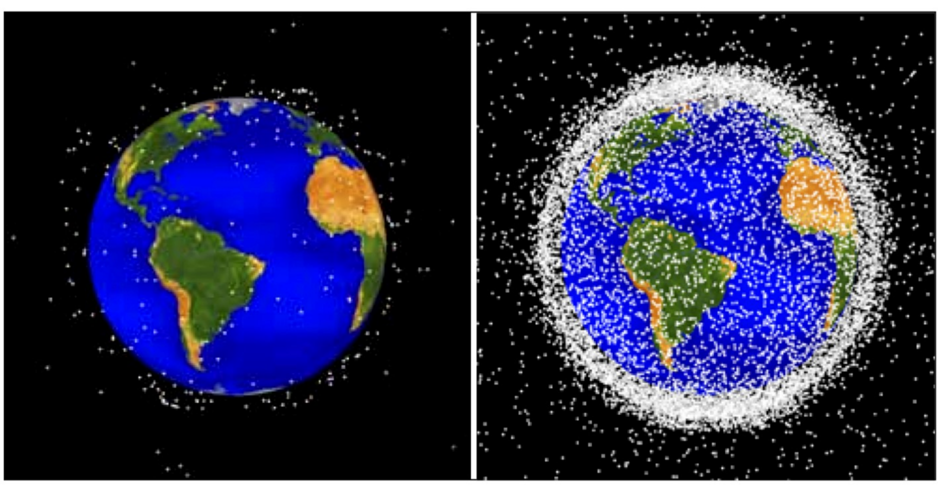

Figure 1.3. Tracked space debris in 1963 and fifty years later

The Earth is now surrounded by tens of thousands of sizeable chunks of debris orbiting at speeds upwards of 17,000 miles per hour. Add to these larger pieces an estimated hundreds of thousands of sub-centimeter-sized artificial particles, and you have got a recipe for potential disaster-for while these small particles may not seem imposing, they can present a serious threat to functional spacecraft.

Active Debris Removal (ADR) is necessary to stabilise the growth of space debris, but even more important is that any newly launched objects comply with post-mission disposal guidelines âĂŞ especially orbital decay in less than 25 years. If this were not the case, most of the required ADR effort would go to compensate for the non-compliance of new objects.

Some actively removing space debris ideas or concepts has been proposed by the researchers and institutions around the world. Japan Aerospace Exploration Agency (JAXA), Euorpean Space Agency and Texas A&M University each presents its own plan.

CHAPTER 2

LITERATURE REVIEW

2.1 Space tether past missions

This chapter is the literature survey on the following topics:

- Space tether past missions
- CubeSat missions with space tether
- Design and construction of:
    1. Space tether deployment/retrieval system
    2. Plasma contactor

It tried to organize the past missions regarding to the space tether and the CubeSat mission in a much clear order. In the same time some historical researches about deployment/retrieval system are listed. The main point is focus on dynamics and control method of tether satellite system.

2.1.1 General tether-related mission

1. NASA

   NASA has been developing tether technology for space applications since the 1960s, including electrodynamic tether propulsion, the Propulsive Small Expendable Deployer System (ProSEDS) flight experiment, âĂİ HangingâĂİ momentum exchange tethers, rotating momentum exchange tethers and tethers supporting scientific space research.

2. NASA-Gemini XI

   The Gemini XI was a manned spaceflight in NASA's Gemini program, launched on September 12,1966. One of the main objectives was related to tethers. It was synoptic terrain photography and a tethered vehicle test. The objectives were all achieved.

3. NASA-Gemini XII

   The Gemini XII was a manned spaceflight in NASA's Gemini program launched on November 11, 1966. One of its major objectives was tethered vehicle evaluation. The objective was achieved.

4. Tethered Payload Experiment (TPE)

   TPE-1mission was launched on January 16, 1980. Its plan was to deploy 400 metres of cable, but its deployed cable was about 38 metres. The TPE-2 mission was launched on 29 January, 1981, and its tether was deployed to a distance about 65 metres. In 1983, the TPE-3, which was also called CHARGE-1, had a length of about 500m. As the deployment system was improved, the tether deployed to its full length of 418 meters, and the tether was also found to act as a radio antenna for the electrical current through the cable. CHARGE-2 was carried out as an international program between Japan and the USA using a NASA sounding rocket at White Sands Missile Range, in December 1985, its tether deployed to a length of 426 metres.

   CHARGE-2B tethered rocket mission was launched in 1992 by NASA with a Black Brant V rocket. The mission was to generate electromagnetic waves by modulating the electron beam. The tether was fully deployed over 400 meters and the experiments all worked as planned.

5. NASA and NDRE-MAIMIK

   The tether length of MAIMIK was about 400m. The mission was designed to study the charging of an electron-beam emitting payload using a tethered mother-daughter payload configuration.

6. US Air Force Geophysics Lab- Echo-7

Designed to study the artificial electron beam propagation along magnetic field lines in space, the mission planned to study how the artificial electron beam propagates along magnetic field lines in space.

7. OEDIPUS

   OEDIPUS-A. The conducting tether was deployed over 985 metres during the flight of a Black Brant sounding rocket in to the auroral ionosphere.

   OEDIPUS-C. The following OEDIPUS mission was the OEDIPUS-C tethered payload mission, which was launched in 1995 with an 1174-metre deployed tether, and a Tether Dynamics Experiment (TDE) was also included as a part of the OEDIPUS-C.

8. Tethered Satellite System (TSS)

   The first orbital flight experiment with a long tether was the Tethered Satellite System (TSS) mission, launched on the Space Shuttle in July 1992. The Tethered Satellite System-1 (TSS-1) was flown during STS-46, aboard the Space Shuttle Atlantis, from July 31 to August 8, 1992. The TSS-1 mission discovered a lot about the dynamics of the tethered system. Although the satellite was deployed only 260 metres, it was able to show that the tether could be deployed, controlled, and retrieved, and that the TSS was easy to control, and even more stable than predicted. The TSS was an electrodynamic tether, its deployment mechanism jammed resulting in tether sever and less than 1000 metres of deployment. The objectives of TSS-1 were

   (a) to verify the performance of the TSS equipment;
   (b) to study the electromagnetic interaction between the tether and the ambient space plasma;
   (c) to investigate the dynamical forces acting on a tethered satellite. In the first tether deployment, when the satellite was moving excessively from side to side, the deployment was aborted. The second trial of deployment was unreeled to a length of 260 metres.

   In 1996, the Tethered Satellite System Reflight (TSS-1R) was carried by using US space shuttle STS-75 successfully. The primary objective of STS-75 was to carry the

Tethered Satellite System Reflight (TSS-1R) into orbit and to deploy it spacewards on a conducting tether.

9. Shuttle Electrodynamic Tether System (SETS)

   The Shuttle Electrodynamic Tether System (SETS) experiment formed part of the scientific experiments comprising the first flight of the NASA/ASI Tethered-Satellite System flown at an altitude of 300 km and at an orbital inclination of 28.5 degrees in July/August 1992. The SETS experiment was designed to study the electrodynamic behaviour of the Orbiter-Tether-Satellite system, as well as to provide background measurements of the ionospheric environment near the Orbiter. The SETS experiment was able to operate continuously during the mission thereby providing a large data set.

10. Small Expendable Deployer System (SEDS)

    The Small Expendable Deployer System-1 (SEDS-1) was launched from Cape Canaveral Air Force Station as a Delta/GPS secondary payload in 1993. SEDS-1 was the first successful 20-kilometre space-tether experiment. When 1 km of tether remained, active braking was applied by wrapping the tether around a "barber pole" brake. Finally, the braking system and sensors did not work as predicted, resulting in hard stop/endmass recoil at deployment completion.

    The Small Expendable Deployer System-2 (SEDS-2) was launched on the last GPS Block 2 satellite in 1994. The SEDS-2 used feedback braking, which was started early in deployment. This limited the residual swing after deployment to 4 degrees. Mission success was defined as deployment of at least 18 km, plus a residual swing angle of less than 15 degrees. The SEDS-2 had an improved braking system compared to SEDS-1, which was a feedback control system and applied braking force as a function of the measured speed of the unrolling tether. This was to ensure that the satellite stopped flying out just when the whole tether was deployed and to prevent the bounces experienced during the previous mission.

11. Plasma Motor Generator (PMG)

    In 1996, the Plasma Motor Generator (PMG) was launched by NASA. This was an electrodynamic tether, which could assess the effectiveness of using hollow cathode assemblies to deploy an ionised gas, and to "ground" electrical currents by discharging the energy to space. An early experiment used a 500 metre conducting tether. When the tether was fully deployed during this test, it generated a potential of 3,500 volts. This conducting single-line tether was severed after five hours of deployment. It was believed that the failure was caused by an electric arc generated by the conductive tether's movement through the Earth's magnetic field. The PMG flight demonstration proved the ability of the proposed Space Station plasma grounding techniques in maintaining the electrostatic potential between the Space Station and the surrounding plasma medium, the ability to use electrostatic tethers to provide thrust to offset drag in LEO space systems and the use of direct magnetic (nonrocket) propulsion for orbital maneuvering.

12. Tether Physics and Survivability Experiment (TiPS)

    The Tether Physics and Survivability Experiment (TiPS) was deployed on June 20, 1996 at an altitude of 1,022 kilometres as a project of the US Naval Research Laboratory. The satellite was a tether physics experiment consisting of two end masses connected by a 4 km nonconducting tether. This experiment was designed to increase knowledge about gravity-gradient tether dynamics and the survivability of tethers in space.

13. The Young Engineers's Satellite (YES)

    The first Young Engineers' Satellite (YES-1) programme was completed on November 3, 1997. It was designed to operate with a 35 km tether deployment, but the mission was cancelled before the flight when the launch authority changed the nominal Ariane orbit. In the new orbit configuration, a deployed 35 km tether would have constituted a hazard to the satellites in LEO.

    The second Young Engineers Satellite (YES2) was launched on September 14, 2007. It was a technology demonstration project designed to test and produce data for the "Space Mail" concept, wherein a tether was used to return material from space to Earth, instead of by conventional chemical propulsion. YES2 aimed to demonstrate a tether-assisted reentry concept, whereby the payload would be returned to Earth using momentum provided from a swinging tether. Deployment was intended to take place in two phases: (1) deployment of 3.5 km of tether to the local vertical and hold and (2) deployment to 30 km for a swinging cut. The measured altitude gain of the Fonton-M3 corresponded with what simulations showed would have happened if 31.7 km of tether were extended, another strong indication that the YES- 2 tether had in fact been fully depolyed.

The YES-2 mission was very nearly a complete success because of the following: (1) the entire record-breaking length of tether has been deployed; (2) Fotino rocket seemed to have been deorbited by using momentum exchange; (3) plentiful data has been gathered on tether deployment, dynamics and deorbiting, which may lead to an operational way of returning capsules without any form of propulsion

14. The Advanced Tether Experiment (ATEx)

    The Advanced Tether Experiment (ATEx) was launched into orbit aboard the National Reconnaissance Office (NRO) sponsored by Space Technology Experiment spacecraft (STEX) on October 3, 1998. ATEx was intended to demonstrate the deployment and survivability of a novel tether design, as well as being used for controlled libration maneuvers. On January 16, 1999, after a deployment of only 22m of tether, ATEx was jettisoned from STEX due to an out-of-limit condition sent by the experiment's tether angle sensor. The ATEx lower end mass was jettisoned from the host spacecraft and the tethered upper and lower end masses freely orbited the Earth in a demonstration of long-term tether survivability.

15. The PICOSAT mission

    The PICOSAT mission was launched on September 30, 2001. It was a real-time tracking satellite of the miniaturized picosatellite satellite series. The name "PICO" combined the first letters of all the four of its experiments, which were the Polymer Battery Experiment (PBEX), the Ionospheric Occultation Experiment (IOX), the Coherent Electromagnetic Radio Tomography (CERTO), and the On Orbit Mission Control (OOMC). A pair of 0.25kg MEMS picosatellites with an intersatellite communications experiment were included in this mission and were connected by a 30 metre tether.

16. Propulsive Small Expendable Deployer System (ProSEDS)–*Cancelled*

The Propulsive Small Expendable Deployer System (ProSEDS) was a NASA space tether propulsion experiment intended to be a follow up to SEDS. It was originally intended to be flown along with a launch of a Global Positioning System (GPS) satellite in the spring of 2003, but was cancelled at the last moment, due to concerns that the tether might collide with the international space station.

17. Multi-Application Survivable Tether (MAST)

    The Multi-Application Survivable Tether (MAST) experiment was launched into LEO on April 17, 2007, in which the 1 km multistrand interconnected tether (Hoytether) was intended to test and prove the long-term survivability of tethers in space, but the tether failed to deploy.

18. Tether Technologies Rocket Experiment (T-REX)

    Tether Technologies Rocket Experiment (T-REX) mission was launched August 31, 2010, on sounding rocket S-520-25, reaching a maximum altitude of 309 km. T-Rex was developed by the Kanagawa Institute of Technology/Nihon University, which led an international team to test a new type of electrodynamic tether (EDT) that may lead to a generation of propellantless propulsion systems for LEO spacecraft. The tether was 300 metres long and deployed as planned, a video of deployment was transmitted to the ground. Tether deployment was verified successfully, as was the fast ignition of a hollow cathode in the space environment.

2.1.2 CubeSat missions with space tether

1. Micro Electro-Mechanical Systems based PicoSat Inspector (MEPSI)

   The MEPSI series (Micro Electro-Mechanical Systems based PicoSat Inspector) was a pair of tethered picosatellites, based on the CubeSat design, launched by a custom deployer aboard the STS-113 Endeavour mission on December 2, 2002. The two spacecrafts were cubic in shape, of mass 1 kg each, and were connected via a 15.2m tether in order to facilitate detection and tracking via ground-based radar.

2. The Space Tethered Autonomous Robotic Satellite (STARS)

On January 23, 2009, a space tether mission called "The Space Tethered Autonomous Robotic Satellite (STARS)," developed by Kagawa Satellite Development Project at Kagawa University, was launched as a secondary payload aboard H-IIA flight. The satellite was named KUKAI after launch and based on a "cubesat" platform like MAST, and consisted of two subsatellites, "Ku" and "Kai," which are linked by a 5-meter tether. The separation of the rocket and satellite and the transfer into the planned orbit were successful, but the tetherâĂŤonly deployed to a length of several centimeters because of the launch lock trouble of the tether reel mechanism .

3. Tether Electrodynamic Propulsion CubeSat Experiment (TEPCE)

   Tether Electrodynamic Propulsion CubeSat Experiment (TEPCE) mission, planned by Naval Research Laboratory, is an electrodynamic tether experiment based on a "triple cubesat" configuration. This experiment is currently planned for launch as a secondary payload in September 2013. Two nearly identical endmasses with a stacer spring between them are used in TEPCE, which separate the endmass and start deployment of a 1 km long braided-tape conducting tether. TEPCE will use a passive braking to reduce speed and hence recoil at the end of electrodynamic current in either direction. The main purpose of this mission is to raise or lower the orbit by several kilometres per day, to change libration state, to change orbit plane, and to actively maneuver.

2.2 Design and construction

2.2.1 Space tether deployment/retrieval system

Besides other operational phases, a TSS mission launch always involves both deployment and retrieval. Tether retrieval is the opposite of deployment and is equally important in dynamical terms. Tether deployment and retrieval are two of the most important steps in space tether applications. The following contents introduce some interesting things about the deployment and retrieval.

1. ATEx design iterations

Mission	Year	Sponsor	Orbit	Length	Status
Gemini XI	1967	NASA	LEO	50 m	Launched
Gemini XII	1967	NASA	LEO	30 m	Launched
TPE-1	1980	NASA/ISAS	Suborbital	400 m	Launched
TPE-2	1981	NASA/ISAS	Suborbital	500 m	Launched
TPE-3 (CHARGE-1)	1983	NASA/ISAS	Suborbital	500 m	Launched
CHARGE-2	1985	NASA/ISAS	Suborbital	500 m	Launched
MAIMIK	1986	NASA/NDRE	LEO	400 m	Launched
ECHO-7	1988	USAF	Suborbital	—	Launched
OEDIPUS-A	1989	NRC/NASA/CRC/CSA	Suborbital	958 m	Launched
CHARGE-2B	1992	NASA/ISAS	Suborbital	500 m	Launched
TSS-1 (STS-46)	1992	NASA/ASI	LEO	267 m	Launched
SEDS-1	1993	NASA	LEO	20 m	Launched
PMG	1993	NASA	LEO	500 m	Launched
SEDS-2	1994	NASA	LEO	20 m	Launched
OEDIPUS-C	1995	NASA/NRC/CRC/CSA	Suborbital	1 km	Launched
TSS-1R (STS-75)	1996	NASA/ASI	LEO	19.6 km	Launched
TSS-2 (STS-75)	1996	NASA	LEO	100 m	Cancelled
TiPS	1996	NRO/NRL	LEO	4 km	Launched
YES	1997	ESA/Delta-Utec	LEO	35 m	Launched
ATEx	1999	NRO/NRL	LEO	22 m	Launched
PICOSATs	2000	Aerospace corporation	LEO	30 m	Launched
MEPSI	2002	Aerospace corporation	LEO	15.2 m	Launched
ProSEDS	2003	NASA	LEO	15 m	Cancelled
MAST	2007	NASA/TUI/Stanford	LEO	1 km	Launched
YES2	2007	ESA/Delta-Utec	LEO	31.7 m	Launched
STARS	2009	Kagawa university	LEO	5 m	Launched
T-REX	2010	ISAS/JAXA	LEO	300 m	Launched
TEPCE	2013	NRO/NRL	LEO	1 km	Planning

Figure 2.1. Tether mission history

In 1997, Koss described the tether deployment mechanism development for the Advanced Tether Experiment (ATEx) mission with some design iterations, which included: energetic(spring) deployment, a DC brush motor-driven deployment mechanism and a stepper motor-driven deployment mechanism

2. Fuzzy-logic feedback deployment control

   A tethered system deployment control by fuzzy-logic feedback was proposed by Licata in 1997, in which the feedback control was based on a simple fuzzy-logic rule and minimal measurements for in-plane tether deployment control problems. The fuzzy-logic law, for the proposed rate feedback control solution to the in-plane deployed tether terminal position-only problem has been associated with the tether length-angle state plane, or the physical deployment trajectory plane.

3. Using Active Reel Type Deplorer to retrieve and deploy tether

Year	Modelling	Problems
1979	Tether-connected two-body systems	General formulation of deployment dynamics considering three-dimensional librational motion, and longitudinal and transverse vibrations
1994	TSS-1	Analysis of the spectra
1995	Non-linear model for tether retrieval	Amplitude of oscillation increasing during retrieval process
1995	Exponential deployment	Dispense with tether alignment without later libration
1997	ATEx	Tether deployment mechanism development
1997	In-plane tether deployment	Fuzzy-logic rule and minimal measurements for deployment control
1998	GATE	Simulation of the retrieval and deployment characteristics
1998	Three-dimensional tether	Deployment considering both in-plane and out-of plane libration
1999	MACE	The close-loop results and insights from the on-orbit control experiments
1999, 2002	Tether-connected satellite systems	Dynamical behaviour during deployment and retrieval process
2003, 2005	Tethered satellites	Various methods for deployment control
2003, 2005	Tethered subsatellite	Optimal control strategy of deployment
2004	Tethered re-entry capsule	Adaptive neural control concept for deployment
2006	3DOF tethered subsatellite system	Optimal control of deployment and retrieval process
2006, 2008	Tethered formation with spinning	Optimal deployment and retrieval
2007	Deployment of space systems	Coupled with long and short tethers
2014	Multiple mass tether	Thrust forces and periods of thruster activation were estimated from various on-ground experiments

Figure 2.2. Summary of tether deployment and retrieval

Carter and Greene studied the simulation of the retrieval and deployment characteristics for the Getaway Tether Experiment (GATE) in 1998. The GATE was a single tether satellite system for the study of tether dynamics and electrodynamic technology. One goal of GATE was to measure and control tether disturbances by micro meteorite impact using an active reel type deplorer, which was able to retrieve and deploy the tether. A closed-loop controller for the tethered system was given, which allowed the tether to be actively reeled in (retrieval) or passively reeled out (deployment), to and from the mother subsatellite.

4. Strategies for TSS retrieval-tension control in the tether

   The dynamical behaviour of tether-connected satellite systems during the deployment and retrieval process was studied by Djebli et al. in 1999 and 2002.The system consisted of a space station connected to a subsatellite by means of a tether of variable length. A simplified model was given in which the space station and the subsatellite were reduced to material points and the system mass centre moved along a circular orbit with three-dimensional transverse and longitudinal oscillations. Strategies for retrieval were obtained in order to increase the tension in the tether at the final stage of retrieval. These laws of retrieval were deduced from the laws obtained in a previous paper for the particular case of a massless tether. Retrieval of a subsatellite to a larger vehicle was examined by Djebli et al. in 2002, which concentrated on laws for retrieval and deployment, combining 'simple' linear and 'fast' laws. This would be applicable to passive momentum exchange tethers and potentially to ED tethers.

   In 2006 and 2008, Williams published his works on the optimal deployment and retrieval for a tethered formation with spinning in the orbital plane, in which a tethered formation was modelled by point mass satellites and connected via inelastic tethers. The optimal deployment and retrieval trajectories using tension control were developed for different spinning conditions.

5. Viscoelastic space billiard model

   In 2003 and 2005, Barkow et al. published three papers on various methods used for controlling the deployment of tethered satellites. The deployment of a tethered satellite system is one of the most critical phases in a tether mission. Based on a viscoelastic space billiard model, a targeting strategy was developed which made use of the system's chaotic nature and allowed the system to be steered into its equilibrium faster and more efficiently, when compared to conventional strategies.

6. Optimal control

   In 2003, Steindl and Troger proposed their works that the optimal control of deployment of a tethered subsatellite moving on a circular orbit around the Earth, in which an optimal control of deployment andretrieval of a tethered subsatellite from a main satellite was treated. Jin et al. presented an optimal control of the deployment and retrieval processes of a three degree of freedom (DOF) tethered subsatellite system using truncated Chebyshev series to approximate the state variables.

7. Adaptive neural control
   An adaptive neural control concept for the deployment of a tethered re-entry capsule was developed by Glabel et al. in 2004, in which the indirect neural controller combined two neural networks, a controller network and a plant model network. After introducing the tether deployment scenario, assumptions and simplifications were applied to the mathematical system model. The simulation results allowed a performance comparison of the linear quadratic regulator and the neural control concept.

8. Tether length factor
   In 2007, Mantri's research aimed to model and understand the deployment of space systems with long and short tethers, which was divided into two parts. The models are set for different length tether systems

9. Spool-type reel using thruster
   In 2014, Iki et al. investigated an ED tether deployment from a spool-type reel using thrusters with a length of several kilomerters, in which the deployment of multiple mass tether deployment was studied the key parameters of a multiple mass tether model. The key parameters of the thrust forces and periods of thruster activation were estimated from various on-ground experiments.

2.2.2 Space tether dynamical modelling

Different models are used for different purposes. In order to solve different problems, several dynamical models have been proposed. Here are the recent proposed models, from 2001 to 2014.

According to the problem, different level models are proposed. From simple to complex, Non-dissipative massive Tether, Electrodynamic Tether(EDT), Tether Satellite SystemïijĹTSSïijĽ, Advanced Safety Tether Operation and ReliabilityïijĹASTORïijĽand Motorized Momentum Exchange TetherïijĹMMETïijĽ are the proposed tether types. According to the problem, researcher can choose the model like slack-sprint model, dumbbell model, flexible model, ponderable tether model, two mass point with the rigid rod model and so on.

Table 2.1. Tether Modeling Method for different problems

Author	**Year**	**Modelling Method**	**What problem to solve**
Cartmell, Ziegler	2001	Scale model of MMET	
Chen and Cartmell, Chen and Ismail	2001-2012	MMET series models	Dynamical modelling and control
Mazzoleni and Hoffman	2001	Tethered artificial gravity satellite	Non-planar spin-up dynamics
Ellis and Hall	2010	Two Point masses connected by rigid rod	Out-of-plane librations
Aslanov	2010	Rigid body TSS system	Plane translational motion and rotational motion
Zanutto et al.	2011	Electrodynamic tether	Perturbed classical three-body problem
Kristiansen et al.	2012	Non-dissipative massive tether	Orbital motions
Zhao et al.	2012	Dumb-bell TSS	Analytical first-order solutions of the librational angles
Jung et al.	2014	TSS with a moving mass	Libration angle with respect to the system parameters

CHAPTER 3

CASE STUDY AND MATLAB SIMULATION IMPLEMENTATION

In this chapter, an specific example[1] of tether satellite system is studied. In this case study, the used dynamic model and Proportional-Differentiation controller are the main analysis focuses. At the end, MATLAB simulation is also implemented.

The tether satellite system consists of two satellite and a tether. The two satellites are named as Target Vehicle and Chaser vehicle which means the task of Chaser vehicle is to capture the target vehicle and to de-rotation of the system. In the real case the target vehicle can be space debris which is moving and rotation around Earth under the gravational force of the Earth. Space debris not only rotates around the Earth, in fact it will also rotate around its body center if any .De-orbiting can be achieved if the energy and angular momentum of space debris consumed. When we let our chaser vehicle connect

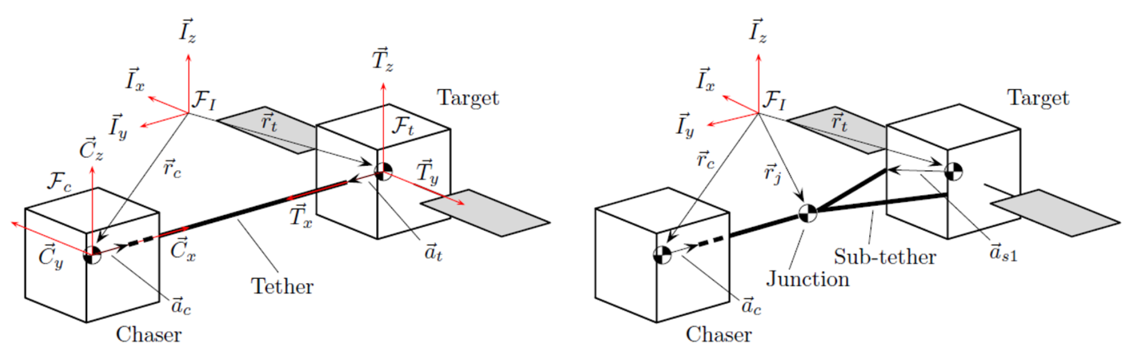

(a) Single tether configuration with reference frame definition.

(b) Sub-tether configuration. For clarity, $\mathcal{F}_c$, $\mathcal{F}_t$, and $\vec{a}_{s2}$ are omitted.

Figure 3.1. Reference frame and vector definition for planar dynamics modeling

with target vehicle using tether, the consumption of angular momentum becomes faster and the deorbiting gets quicker. So we can say that chaser vehicle plays as a role of active debris remover.

Using different kind of tether configuration, the effect of deorbiting target vehicle can be quite different.In Hovell's article, single tether confguration and sub-tether configuration are compared. The sub-tether configuration is like harpoon. The main tether links the Chaser vehicle with the junction point, which will be modeled as a point mass later.Two seperate tethers link the junction and Target vehicle. The proposed sub-tether configuration can enhance the deorbiting mechanism, reducing the target tether angle and angular rate of target and finally dissipating angular momentum from the system much more quickly.

3.1 Physical Model Assumption

1. Massless tether, Constant end-body mass and visco-elastic tether

   The tether is assumed as massless since it is much more lighter than end-body satellites. The single tether and sub-tether are modeled as nonlinear spring. The spring force are related to tether stretch and the relationship is set as visco-elastic.

2. Three degree of freedom for Chaser vehicle and Target vehicle

   Only three degree of freedom is considered in this case which means the satellite can only do translational motion along X axis and Y axis and rotational motion about the Z axis. This assumption makes the dynamics modeling of satellite much easier. The two satellites, target and chaser, are at the same level height which means there is no translational motion along Z axis i.e the z = 0. Similarly, the rotational motion about X axis and the rotational motion about Y axis are not con

3. No external forces applied to the center of mass of the whole tethered satellite system

   In the tether satellite system, the force of tether and the chaser's control force are force source. No external force, such as gravational force and distrubance force applied to the center of mass of the whole system.

4. The Inertia matrix is constant

5. Body frame of each of the end-masses is aligned with the principal axes of the end-masses

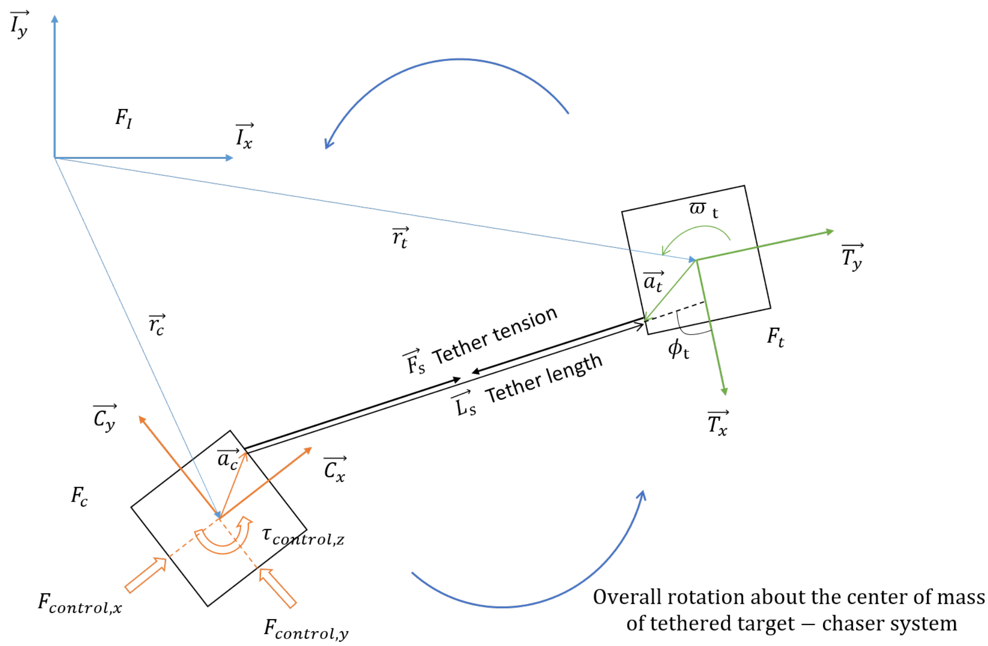

Figure 3.2. Definition of the Inertial frame, Chaser body frame and Target body coordinate systems

There are three coordinate systems defined in the article and all of them are defined as right-handed system. Between two different coordinate systems the attitude matrix $A(\theta)$ is the transformation matrix whcih used to rotate the vector components from a body frame to Inertial frame.

$$A(\theta) = \begin{bmatrix} \cos(\theta) & -\sin(\theta) \\ \sin(\theta) & \cos(\theta) \end{bmatrix}$$

The point where tether attached the Chaser vehicle or Target vehicle is called attached point. This point is fixed in the body frame so that we can use tether attachment vector with respect to the body centor of mass to describe this attach point. The tether attachment vector is denoted as a. The attitude θ of a body frame (F_C for the chaser or F_T for of the target) is the angle of rotation between the body frame relative to the Inertial frame F_I about the z-axis where the z-axis of all inertial and body frames are parallel. The transformation of vectors from body frame to Inertial frame is using the equation $\mathbf{x_I} = A(\theta)\mathbf{x_b}$ which I means Inertial frame and b means body frame.

1. Reference inertial frame $\mathsf{F_I}$ Coordinates

$$\mathbf{I} = [\mathbf{I}_x, \mathbf{I}_y, \mathbf{I}_z]$$

$\mathsf{F_I}$ is fixed. The position of origin point and direction of three axes will not change with time.

2. Reference inertial frame $\mathsf{F_T}$ Coordinates

$$\mathbf{T} = [\mathbf{T}_x, \mathbf{T}_y, \mathbf{T}_z]$$

$\mathsf{F_T}$ denotes the Target body-fixed frame. The origin point of **T** is at the center of mass of the Target vehicle. The x axis of $\mathsf{F_T}$ is pointed to the chaser at the beginning.

3. Reference inertial frame $\mathsf{F_C}$ Coordinates

$$\mathbf{C} = [\mathbf{C}_x, \mathbf{C}_y, \mathbf{C}_z]$$

$\mathsf{F_C}$ denotes the Chaser body-fixed frame.The origin point of **C** is at the center of mass of the Target. The x axis of $\mathsf{F_C}$ is pointed to the target at the beginning.

3.2 Motion governing equation and Physics model for the system

This section talks about the details of physical model and the motion governing equation

3.2.1 Motion governing equation

The governing equations are Newton's second law and Euler's equation.

Using the Newton's second law we can get that the sum of force vector components acting on any body in Inertia Frame,**F**, equals the mass of the satellite m times the resulting acceleration vector components in Inertia Frame $\ddot{r}$ i.e. $\mathbf{F} = m\ddot{\mathbf{r}}$

Similarly, using the Euler's equation we can get that the torque of the chaser's body or target's body as a result of the force exerted by the tether and/or the chaser's control actuator equals z axis Principal moment of inertia multiplied by Angular velocity of an end-mass/satellite relative to the inertial frame (which also equals to the angular velocity relative the body frame) i.e. $J_{zz}\dot{\omega} = \tau_z$

3.2.2 Physics model for the system

The whole system is modeled as a nonlinear stiffness spring-damper system. The damping coefficient of the damper is constant. The tether is made of 56% polyester and 44% rubber. The spring constant k has strong nonlinearity.

- The spring constant changes as the extension of tether change
- When tether is extended, the spring force $F_{spring} = k \times$(length of stretched tether - tether natural length)
- $F_{spring} = 0$ when tether is slacked

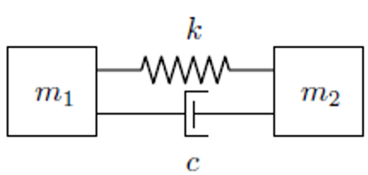

Figure 3.3. System model

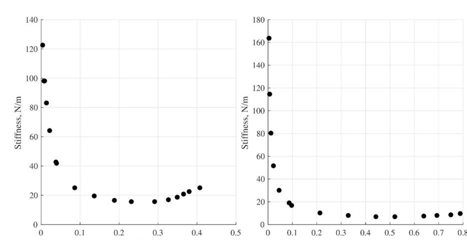

Figure 3.4. Stiffness stetch relation

3.2.3 Force and Torque analysis

1. For the Target vehicle, it only received the force of tether tension which denoted as $-\overrightarrow{F_S}$. The torque τ_t is the torque made by tether tension about the center of mass of the target body.

$$\tau_t = a_{t,y}F^t_{s,x} - a_{t,x}F^t_{s,y}$$

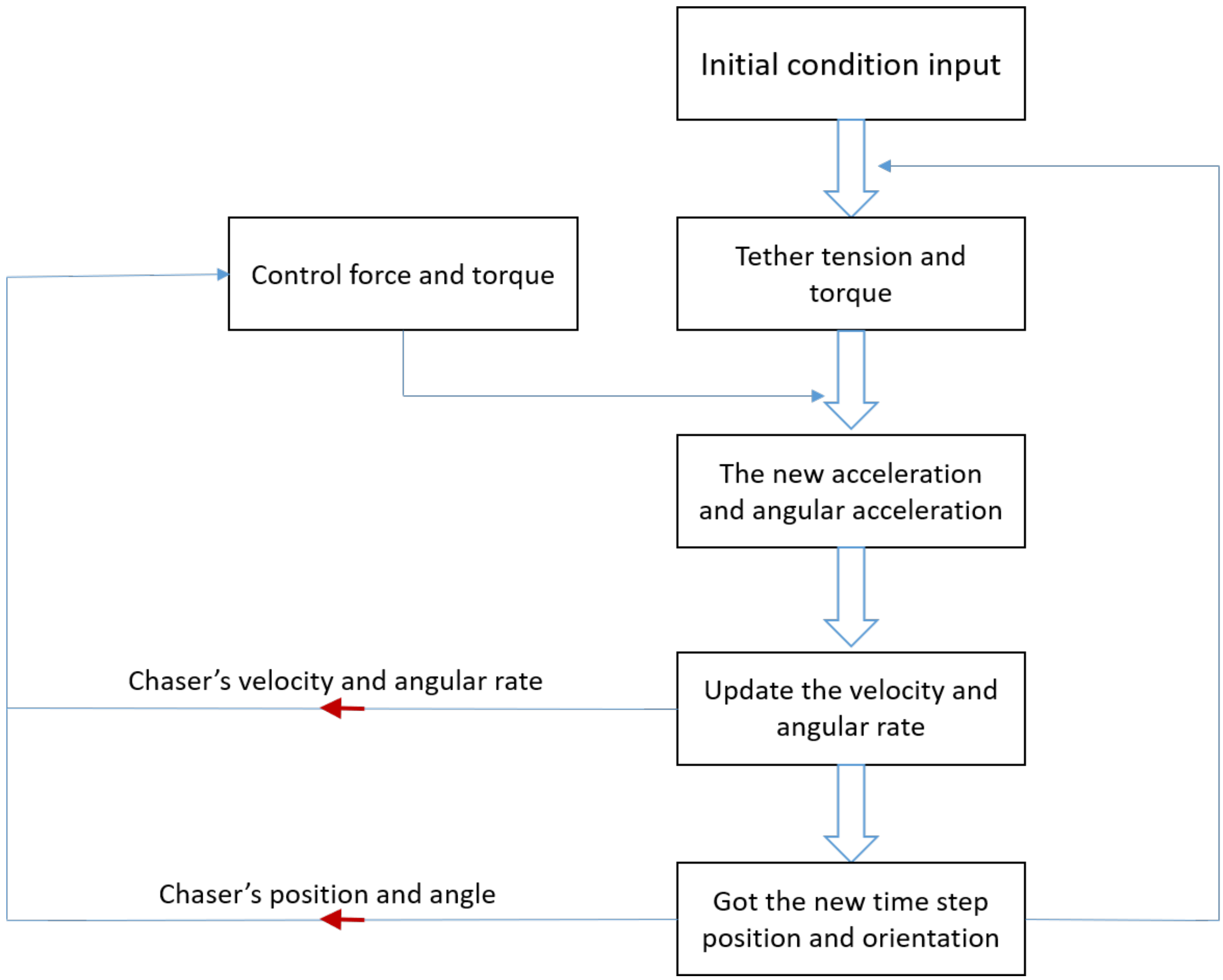

Figure 3.5. Flowchart of the calculation process

F_s^t is the tether force expressed in F_t i.e. $F_s^t = A(\theta_t)^T F_S$
$F_{s,x}^t, F_{s,y}^t$ are the x and y components of F_s^t in F_T, respectively.

2. For the Chaser vehicle tether force $\overrightarrow{F_S}$ and active control force $\overrightarrow{F_{control}}$ both exist. The torque also consists of two parts $\tau_{control}$ and τ_c. The $\tau_{control}$ and $\overrightarrow{F_{control}}$ are the active control way that research can design in order to get the better deorbiting performance.

$$\tau_c = a_{c,x} F_{s,x}^c - a_{c,y} F_{s,x}^c$$

F_s^c is the tether force expressed in F_c i.e. $F_s^c = A(\theta_c)^T F_S$
$F_{s,x}^c, F_{s,y}^c$ are the x and y components of F_s^c in F_c, respectively.

3.2.4 Tether length, tether tension and tether torque

According to Figure3.2, changing all the vectors in the Inertial frame then the vector form of tether length can be written as follows:

$$\overrightarrow{L_S} = -(\overrightarrow{r_c} + A(\theta_c)\overrightarrow{a_c}) + (\overrightarrow{r_t} + A(\theta_t)\overrightarrow{a_t})$$

As Figure 3.3 described before, the damping mechanism of tether results in the damping force: $c(\Delta\overrightarrow{v} \cdot \frac{\overrightarrow{L_S}}{\left\|\overrightarrow{L_S}\right\|})$. It results from damping factor times the velocity change in the tether's direction

The tether tension is:

$$\overrightarrow{F_S} = \left(k(\left\|\overrightarrow{L_S}\right\| - L_{s,nature}) + c(\Delta\overrightarrow{v} \cdot \frac{\overrightarrow{L_S}}{\left\|\overrightarrow{L_S}\right\|})\right)\frac{\overrightarrow{L_S}}{\left\|\overrightarrow{L_S}\right\|}$$

$\frac{\overrightarrow{L_S}}{\left\|\overrightarrow{L_S}\right\|}$ is the unit vector of the tether.$\Delta\overrightarrow{v}$ is the difference of the time derivative of two body's absolute postion.

$$\Delta\overrightarrow{v} = \frac{d}{dt}(\overrightarrow{r_t} + A(\theta_t)\overrightarrow{a_t}) - \frac{d}{dt}(\overrightarrow{r_c} + A(\theta_c)\overrightarrow{a_c}) = \overrightarrow{v_t} + \frac{d}{dt}(A(\theta_t))\overrightarrow{a_t} - \overrightarrow{v_c} - \frac{d}{dt}(A(\theta_c))\overrightarrow{a_c}$$

Since the derivate is used for the angle, we can rewrite the $\frac{d}{dt}(A(\theta_t))\overrightarrow{a_t}$ in terms of angular rate and tether attachment vector.

$$\frac{d}{dt}(A(\theta_t))\overrightarrow{a_t} = \frac{d}{dt}\left(\begin{bmatrix}\cos(\theta_t) & -\sin(\theta_t)\\ \sin(\theta_t) & \cos(\theta_t)\end{bmatrix}\right)\overrightarrow{a_t} = \begin{bmatrix}\cos(\theta_t) & -\sin(\theta_t)\\ \sin(\theta_t) & \cos(\theta_t)\end{bmatrix}\begin{pmatrix}-\omega_t a_{t,y}\\ \omega_t a_{t,x}\end{pmatrix}$$

which means that

$$\tfrac{d}{dt}(A(\theta_t))\overrightarrow{a_t} = A(\theta_t)\begin{pmatrix}-\omega_t a_{t,y}\\ \omega_t a_{t,x}\end{pmatrix} \tfrac{d}{dt}(A(\theta_c))\overrightarrow{a_c} = A(\theta_c)\begin{pmatrix}-\omega_c a_{c,y}\\ \omega_c a_{c,x}\end{pmatrix}$$

Tether torque can be written as the time derivative of system angular momentum. It equals the time derivative of system angular momentum with regard to the relative moving coordinate system plus the moving frame's absolute angular velocity times the

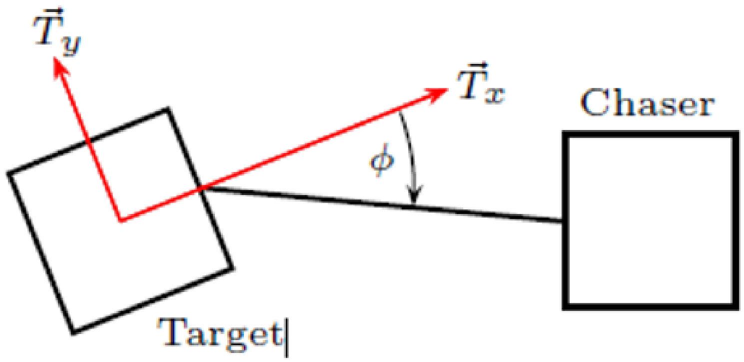

Figure 3.6. Positive tether target angle

angular momentum. In this case the moving frame just has translational motion in Inertia frame. The moving frame's absolute angular velocity doesn't exist in this case.

$$M = \frac{dH}{dt} = \dot{H}_{relative} + \Omega \times H = \dot{H}_{relative} = \frac{J_{zz}\omega}{dt} = J_{zz}\dot{\omega}$$

The torque in Inertial frame equals the torque in body frame. For the rigid body i In the inertial frame, the euler's equation gives us the relationship between the exerted torque τ and resulted angular acceleration $\dot{\omega}$ .i.e. $J_i\dot{\omega} + \omega_i \times J_i\omega_i = \sum \tau$

According to the assumption 3.1 we can simplified the Euler's equation as: $J_{izz}w_{iz} = \tau_{iz}$ i can be c for chaser or t for target. $\tau = a_i \times F_S^i$ $\tau_t = a_{t,y}F_{s,x}^t - a_{t,x}F_{s,y}^t$ $\tau_c = a_{c,x}F_{s,x}^c - a_{c,y}F_{s,x}^c$

3.3 Control goal of Chaser vehicle

To archieve the goal of deorbiting target satellite, the Chaser vehicle need to regulate and reduce the angle between tether and target so as to make the tether aligned with the target or force Chaser and target has the parellel surface. To reduce the angular rate of target vehicle, dissipate angular momentume from the system and at last make the target go to lower altitude orbit. The easiest way is to use the proportional-derivative controller for the position and altitude contro of the tether. The force controller uses the difference between desired chaser radius vector and actual chaser radius vector as the feedback signal.

The force $\overrightarrow{F_{s,control}}$ equals $\mathbf{K_P}\left[\overrightarrow{r_{des}(t)} - \overrightarrow{r_c(t)}\right] + \mathbf{K_D}\left[\overrightarrow{\dot{r_{des}}(t)} - \overrightarrow{\dot{r_c}(t)}\right]$ Similarly the torque controller uses the desired chaser attitude angle and actual chaser attitude angle as the control feedback signal.

$$\tau_{control} = K_{P,\theta}\left[\theta_{des}(t) - \theta_c(t)\right] + K_{D,\theta}\left[\dot{\theta_{des}}(t) - \dot{\theta_c}(t)\right]$$

$K_P, K_{P,\theta},, K_D, K_{D,\theta}$ are the Proportional gain matrix and the Derivative gain matrix respectively. These matrix value are designed and tuned by designer for the special case.

3.4 MATLAB Implementation

In this section, the MATLAB simulation case is implemented. To simplified the study, the implementation case use only one controller. The thrust stabilization only use force controller. The Tether Satellite System Spin Stabilization only use torque control, commanding the chaser to continually point its C_x axis toward the target. In the real case the controller can be the combination of these two kinds. Here we just implemented the Thrust stabilization of single tether for illustration the problem.

The detail MATLAB code is in the Appendix. Symbols have the same meaning and constant values are not changed, as[1].

3.5 Thrust stabilization

The chaser is designed as uniformly accelerated motion for simplicity. The motion can be replayced by any other arbitarily defined motion.

$$\overrightarrow{r_{des}(t)} = \overrightarrow{r_0} + \overrightarrow{d}\frac{t^2}{2}$$

d is the acceleration got from the desired final radius vector, the initial radius vector and assigned time for motion, $\overrightarrow{d} = \frac{2(\overrightarrow{r_{final}} - \overrightarrow{r_0})}{t^2}$. $\overrightarrow{\dot{r_{des}}(t)} = \overrightarrow{d}t$

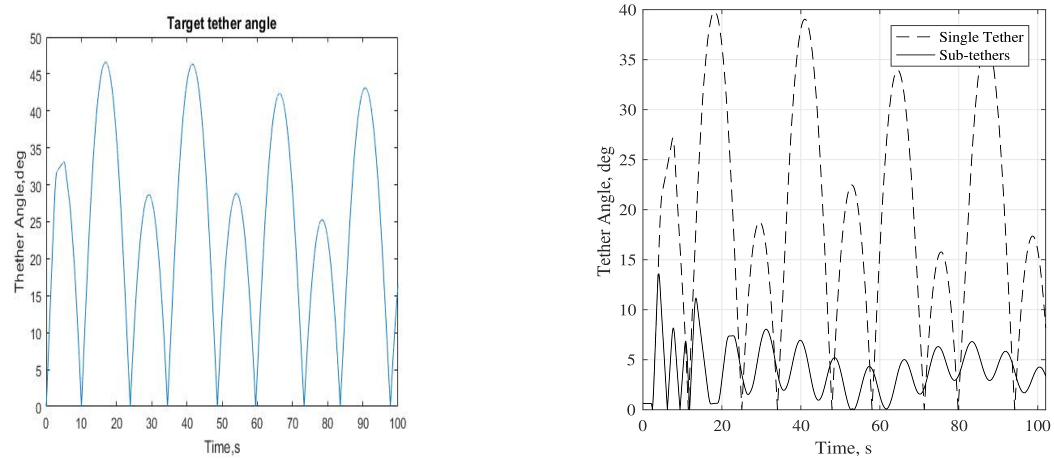

Figure 3.7. Comparison of Target tether angle. Left: Kaiwen Right: Hovell

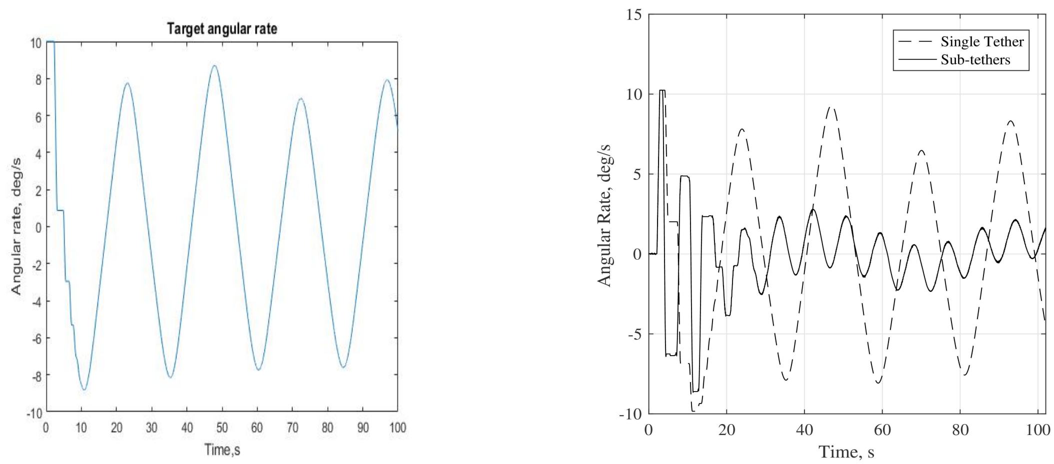

Figure 3.8. Comparison of Target angular rate. Left: Kaiwen Right: Hovell

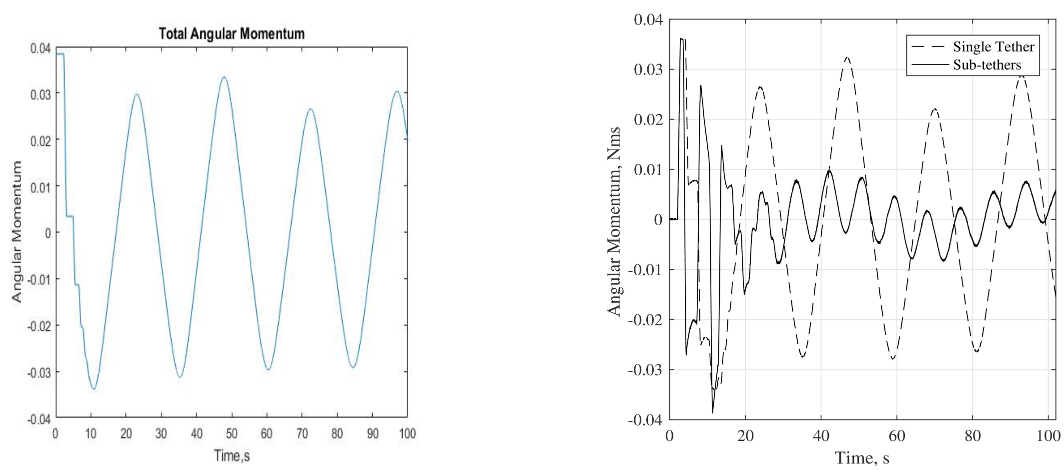

Figure 3.9. Comparison of Total angular momentum. Left: Kaiwen Right: Hovell

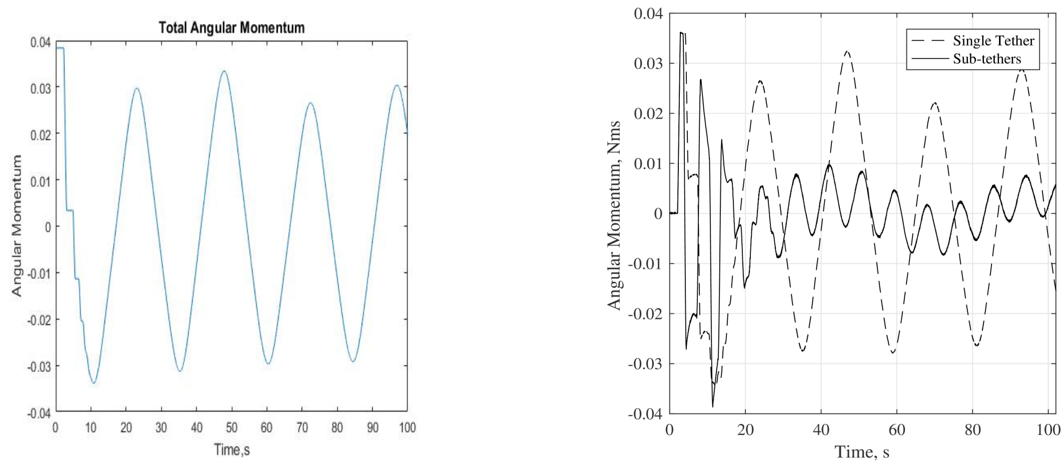

Figure 3.10. Comparison of Total angular momentum. Left: Kaiwen Right: Hovell

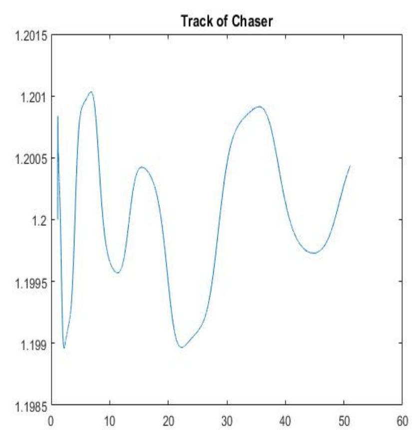

Figure 3.11. Track of Chaser

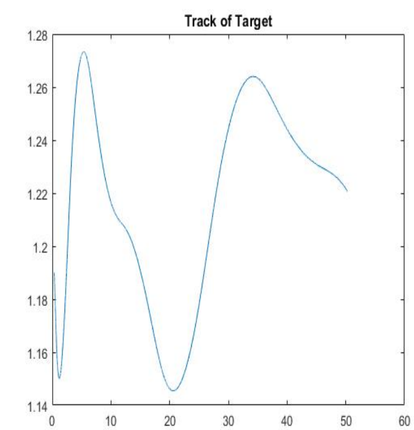

Figure 3.12. Track of Target

CHAPTER 4

APPENDIX

4.1 MATLAB

```
% This code is an implementation of Thrust Stabilization
% for single tether
% Hovell, K, and Ulrich, S. (2017)
% "Experimental Validation for Tethered Capture of the Spinning
   Space Debris"
% AIAA SciTech Forum, AIAA Guidance, Navigation, and Control
   Conference, Grapevine, Texas. 9 ?13 January
% Paper no AIAA 2017−1049.

% ======
% Nomenclature:
% Jzzt = Moment of inertia, target about z−axis
% Jzzc = Moment of inertia, chaser about z−axis

% mt = Mass of the target
% mc = Mass of the chaser
% mj = Mass of the junction

% thetac0 = Initial angle of the chaser
% thetat0 = Initial angle of the target

% TS = Time step

% Lm0= unstretched length of the main tether
% Ls10 = unstretched length of the sub tether 1
% Ls20 = unstretched length of the sub tether 2
% Ls0 = unstretched length of the single tether

% ac = tether attachment point to body chaser with respect to
   chaser's
% center of mass
% as1 = tether attachment point to body sub tether 1 with respect
    to
% sub−tether1's center of mass
```

```
% as2 = tether attachment point to body sub tether 2 with respect
    to
% sub−tether2 's center of mass
% at = tether attachment point to body target with respect to
% target 's center of mass

% csingle = damping coefficient for single tether
% csub = damping coefficient for sub tether

% KPtheta = proportional gain matrix for the theta
% KDtheta = derivative gain matrix for the theta
% KP = proportional gain matrix for the position
% KD = derivative gain matrix for the postion

% ======
% Define initial conditions and TSS parameters for all
   simulations and
% ïijŽexperiment

%in ÂůKgm^2
Jzzt=0.22;
Jzzc=0.30;

%in Kilogram
mt=12.19;
mc=17.24;
mj=0.01;

%in Degree
thetac0=180;
thetat0=0;

% in Second
TS=0.004;

%in Meter
Lm0=0.28;
Ls10=0.28;
Ls20=0.28;
Ls0=0.54;
ac=[0.135;−0.009];
as1=[0.110;0.127];
as2=[0.113;−0.094];
at=[0.110;0.016];
```

```
% in ÂůNewtonsecond/meter
csingle=3.0;
csub=0.9;

KPtheta=0.33;
KDtheta=0.56;
KP=[19.1 0;0 19.1];
KD=[32.7 0;0 32.7];

% ======
% Define initial conditions for Thurst Stabilization simulations
  and experiment
rt0=[0.35;1.19];
rc0=[1.10;1.20];
vt0=[0;0];
vc0=[0;0];
wt0=10; %degree/second
rf=[3.10;1.20];

% ======
% Initialization
% Simulation at time t=2s
% Nothing change in the first two seconds
rt=rt0;
rc=rc0;
vt=vt0;
vc=vc0;
thetat=thetat0;
thetac=thetac0;
Ls=rt+A(thetat)*at-rc-A(thetac)*ac;

% fai is the target tether angle
fai=norm(atand(Ls(2)/Ls(1))-thetat);



wt=wt0;
wc=0;
t=0; % It started to simulate at T=2, which seem it as t=0;
Fs=[0;0];

% AngularMomentum
% In radius
```

```
AngularMomentum = Jzzt * wt/57.3 + Jzzc * wc/57.3 ;

accelerationc=[0;0];
accelerationt=[0;0];
angularaccelerationt=0;
taot=0;
Fcontrol=[0;0];



for i=1:25000 % i* TS = the time , i is the number of the current
    time step
%record the data
recordt(i)=t;
recordrc(i,1)=rc(1);
recordrc(i,2)=rc(2);
recordrt(i,1)=rt(1);
recordrt(i,2)=rt(2);
recordthetat(i)=thetat;

recordwt(i)=wt;
recordFs(i,1)=Fs(1);
recordFs(i,2)=Fs(2);

recordLs(i,1)=Ls(1);
recordLs(i,2)=Ls(2);


recordvc(i,1)=vc(1);
recordvc(i,2)=vc(2);

recordvt(i,1)=vt(1);
recordvt(i,2)=vt(2);

recordaccelerationc(i,1)=accelerationc(1);
recordaccelerationc(i,2)=accelerationc(2);
recordaccelerationt(i,1)=accelerationt(1);
recordaccelerationt(i,2)=accelerationt(2);

recordangularaccelerationt(i)=angularaccelerationt;

recordtaot(i)=taot;

recordFcontrol(i,1)=Fcontrol(1);
recordFcontrol(i,2)=Fcontrol(2);
```

```
recordfai(i)=fai;

recordAngularMomentum(i) = AngularMomentum ;

%recordstiffness(i) = stiffness(norm(Ls)-Ls0);

%Ls is the vector which is from chaser to target, pointing at the
    target
Ls=rt+A(thetat)*at-rc-A(thetac)*ac;

% fai is target tether angle
fai=norm(-atand(Ls(2)/Ls(1))+thetat);


% Calculate the state of the tether
% Hovell and Ulrich (2017) eqn 19
if (norm(Ls)-Ls0)>0 % tether is tensioned
    Fs=(stiffness(norm(Ls)-Ls0)*(norm(Ls)-Ls0)+...
        dot(csingle*(vt+A(thetat)*[-wt/57.3*at(2);wt/57.3*at(1)]-
           vc-A(thetac)*[-wc/57.3*ac(2);wc/57.3*ac(1)]),...
        Ls/norm(Ls))).*Ls/norm(Ls);
else % tether is slackness
    Fs=[0;0];
end

% Force on target due to tether tension:
% through center of mass
% referenced to the target's body frame
Fst=(A(thetat))'*Fs;
Fsc=(A(thetac))'*Fs;


% Torque on target due to tether tension:
% about the z-axis of body frame (which is parallel to the z-axis
    of inertial frame)
% through center of mass target
% referenced to target body frame (the torque referenced to the
   body is the same as to the inertial frame)
taot=at(2)*Fst(1)-at(1)*Fst(2); % Nm
taoc=ac(1)*Fsc(2)-ac(2)*Fsc(1); % Nm

% The control thrust of chaser vehicle
Fcontrol=KP*(rdes(t)-rc)+KD*(vdes(t)-vc);

% The control torque of chaser vehicle
```

```
taocontrol=KPtheta* (180 - thetac) + KDtheta*(0-wc)   ;
accelerationt=(-Fs/mt);
accelerationc=(Fs+Fcontrol)/mc;
angularaccelerationt=taot/Jzzt;
angularaccelerationc=(taoc+taocontrol)/Jzzc;

% position and angle update
rt=rt+vt*TS;
rc=rc+vc*TS;
thetat=thetat+wt*TS;
thetac=thetac+wc*TS;

vt=vt+accelerationt*TS;
wt=wt+angularaccelerationt*TS*(180/pi);%/degree t-1
vc=vc+accelerationc*TS;
wc=wc+angularaccelerationc*TS*(180/pi); %/degree t-1
AngularMomentum = Jzzt * wt/57.3 + Jzzc * wc/57.3;
t=t+TS;
end
recordt=recordt';
recordthetat=recordthetat';
recordwt=recordwt';


recordrc=recordrc';
recordrt=recordrt';
recordvc=recordvc';
recordvt=recordvt';
recordaccelerationc=recordaccelerationc';
recordaccelerationt=recordaccelerationt';
recordangularaccelerationt=recordangularaccelerationt';
recordangularaccelerationt=recordangularaccelerationt';
recordaccelerationc=recordaccelerationc';
recordaccelerationt=recordaccelerationt';
recordtaot=recordtaot';
recordFcontrol=recordFcontrol';

n=1;
figure(n)
plot(recordt,recordwt);
title('Target angular rate')
xlabel('Time,s')
ylabel('Angular rate, deg/s')
n=n+1;
```

```
figure(n)
plot(recordt,recordthetat)
title('angle of target')
n=n+1;

figure(n)
plot(recordt,recordrc(1,:))
title(' x position of the chaser')
n=n+1;

figure(n)
plot(recordt,recordrc(2,:))
title('y position of the chaser')
n=n+1;

figure(n)
plot(recordt,recordrt(1,:))
title('x position of the target')
n=n+1;

figure(n)
plot(recordt,recordrt(2,:))
title('y position of the target')
n=n+1;

figure(n)
plot(recordt,mod(recordfai,360))
title('Target tether angle')
xlabel('Time,s')
ylabel('Thether Angle,deg')
n=n+1;

figure(n)
plot(recordt,recordAngularMomentum)
title('Total Angular Momentum')
xlabel('Time,s')
ylabel('Angular Momentum')

n = n + 1;
figure(n)
plot(recordrc(1,:),recordrc(2,:))
title('Track of Chaser')

n = n+1;
figure(n)
```

```
plot(recordrt(1,:),recordrt(2,:))
title('Track of Target')

% The function gives the attitude matrix in terms of theta
% cos -sin; sin cos;

function attitude=A(sita)
attitude=[cosd(sita) -sind(sita);sind(sita) cosd(sita)];
end

% calculate the design radius vector of time t
% the goal is to reach the destination in 20s after t=2
function [rdes]=rdes(t)
rc0=[1.10;1.20];
rf=[3.10;1.20];
d=2.*(rf-rc0)./(20*20); %in 20s
[rdes]=(rc0+d.*(t*t/2));
end

% calculate the single tether stiffness(N/m) in terms of
% stretch(m)-independent variable
% x=(||Ls||-Ls,0)
function stiff=stiffness(x)
originalstiffness
   =[163.500000000000,114.450000000000,80.2636363636363,51.3857142857143,29.

originalstretch
   =[0.00300000000000000,0.00600000000000001,0.0110000000000000,0.02100000000

stiff=spline(originalstretch,originalstiffness,x);
end

% calculate the design velocity of time t
% the goal is to reach the destination in 20s after t=2s
function vdes=vdes(t)
rc0=[1.10;1.20];
rf=[3.10;1.20];
d=2.*(rf-rc0)./(20*20); %in 20s
vdes=d*t;
end
```

4.2 Arduino CSV Streaming Example

```
#include <ArdusatSDK.h>
```

```
#include <Wire.h>
#include <Arduino.h>


/*-----------------------------------------------------------------------
 *  Setup Software Serial to allow for both RF communication and
    USB communication
 *    RX is digital pin 8 (connect to TX/DOUT of RF Device)
 *    TX is digital pin 9 (connect to RX/DIN of RF Device)
 *-----------------------------------------------------------------------
ArdusatSerial serialConnection(SERIAL_MODE_HARDWARE_AND_SOFTWARE,
    8, 9);

/*-----------------------------------------------------------------------
 *  Constant Definitions
 *-----------------------------------------------------------------------


Acceleration accel;
Gyro gyro;
Magnetic mag;
Orientation orient(accel, mag);

void setup(void) {
  serialConnection.begin(57600);

  accel.begin();
  gyro.begin();
  mag.begin();
  orient.begin();
  serialConnection.println("Start of the loop");
  serialConnection.println("The acceleration x y z unit in m/s
     ^2");
  serialConnection.println("The angular rate x y z unit in radian
      per second");
  serialConnection.println("The orientation roll pitch heading
     unit in degree");
}

void loop(void) {
  serialConnection.println(accel.readToCSV("Acceleration"));
  serialConnection.println(gyro.readToCSV("Gyro"));
```

```
  serialConnection.println(orient.readToCSV("Orientation"));
}
```

4.3 MATLAB Serial REALTIME PLOTING

```
%% Pre-process
close all;  % close all figures
clear all;  % clear all workspace variables
clc;        % clear the command line
fclose('all'); % close all open files
delete(instrfindall); % reset com port

%% Constatns
BAUDRATE = 57600; % Need to configure Xbee parts BD i.e.
   Interface Data Rate
INPUTBUFFER = 51200; %Unit in bytes. Definition:A location that
   holds all
% incoming information before it continues to the CPU for
   processing;
% Buffers used to store information before it processed


%% Initialize the stripchart
figure_acceleration = figure('Name','Acceleration');
axes_accelerationx = subplot(3,1,1); % Axes Object
xlabel(axes_accelerationx,'Time/ second')
ylabel(axes_accelerationx,'Accelerationx/ m/s^2')

axes_accelerationy = subplot(3,1,2);
xlabel(axes_accelerationy,'Time/ second')
ylabel(axes_accelerationy,'Accelerationy/ m/s^2')

axes_accelerationz = subplot(3,1,3);
xlabel(axes_accelerationz,'Time/ second')
ylabel(axes_accelerationz,'Accelerationz/ m/s^2')

h_ax = animatedline(axes_accelerationx,'MaximumNumPoints',Inf,'
   Marker','o','Color','red'); % animated line object
h_ay = animatedline(axes_accelerationy,'MaximumNumPoints',Inf,'
   Marker','+','Color','blue');
h_az = animatedline(axes_accelerationz,'MaximumNumPoints',Inf,'
   Marker','*','Color','green');

figure_gyro = figure('Name','Gyro');
```

```
axes_gyrox = subplot(3,1,1);
xlabel(axes_gyrox,'Time/ second')
ylabel(axes_gyrox,'Gyrox/ rad/s')

axes_gyroy = subplot(3,1,2);
xlabel(axes_gyroy,'Time/ second')
ylabel(axes_gyroy,'Gyroy/ rad/s')

axes_gyroz = subplot(3,1,3);
xlabel(axes_gyroz,'Time/ second')
ylabel(axes_gyroz,'Gyroz/ rad/s')

h_gx = animatedline(axes_gyrox,'MaximumNumPoints',Inf,'Marker','o
    ','Color','red');
h_gy = animatedline(axes_gyroy,'MaximumNumPoints',Inf,'Marker
    ','+','Color','blue');
h_gz = animatedline(axes_gyroz,'MaximumNumPoints',Inf,'Marker
    ','*','Color','green');

figure_orientation = figure('Name','Orientation');
axes_roll = subplot(3,1,1);
xlabel(axes_roll,'Time/ second')
ylabel(axes_roll,'Roll/ deg')

axes_pitch = subplot(3,1,2);
xlabel(axes_pitch,'Time/ second')
ylabel(axes_pitch,'Pitch/ deg')

axes_heading = subplot(3,1,3);
xlabel(axes_heading,'Time/ second')
ylabel(axes_heading,'Heading/ deg')

h_roll = animatedline(axes_roll,'MaximumNumPoints',Inf,'Marker','
    o','Color','red');
h_pitch = animatedline(axes_pitch,'MaximumNumPoints',Inf,'Marker
    ','+','Color','blue');
h_heading =animatedline(axes_heading,'MaximumNumPoints',Inf,'
    Marker','*','Color','green');

% Index
i = 1;
j = 1;
k = 1;

% Record the data
```

```
% 10000 Row data
record_acceleration = zeros(10000,4);
record_gyro = zeros(10000,4);
record_orientation = zeros(10000,4);

%% Create a serial object
board = serial('COM4','BaudRate',BAUDRATE,'DataBits',8);
% Related with the used COM, can be different
% COM4 for wireless, COM3 for wire
% BAUDRATE unit: bits per second, e.g. 9600 means 9600 bits per
   second,
% i.e. 1200 bytes per second i.e. 1.2 KB/s or 1.17KB/s


% Set serial port buffer
set(board,'InputBufferSize',INPUTBUFFER);
% InputBufferSize: total number of bytes that can be stored in
   the input
% buffer during a read operation. The read operation is
   terminated if the
% amount of data stored in the input buffer equals the
   InputBufferSize

fopen(board);
while(1)
    a = fgetl(board);% a:character vector
    b = textscan(a,'%u32 %s %f %f %f %u32','Delimiter',',');

    if strcmp(char(b{2}),'Acceleration')

        time = double(b{1})/1000; % in second
        ax = b{3};
            addpoints(h_ax,time,ax);
            drawnow limitrate

        ay = b{4};
            addpoints(h_ay,time,ay);
            drawnow limitrate

        az = b{5};
            addpoints(h_az,time,az);
            drawnow limitrate

        record_acceleration(i,:)=[time ax ay az];
        i=i+1;
```

```
    elseif strcmp(char(b{2}),'Gyro')
        time = double(b{1})/1000; % in second
        gx = b{3};
            addpoints(h_gx,time,gx);
            drawnow limitrate

        gy = b{4};
            addpoints(h_gy,time,gy);
            drawnow limitrate
        gz = b{5};
            addpoints(h_gz,time,gz);
            drawnow limitrate

        record_gyro(j,:)=[time gx gy gz];
        j=j+1;

    elseif strcmp(char(b{2}),'Orientation')
        time = double(b{1})/1000; % in second
        roll = b{3};
            addpoints(h_roll,time,roll);
            drawnow limitrate

        pitch = b{4};
            addpoints(h_pitch,time,pitch);
            drawnow limitrate

        heading = b{5};
            addpoints(h_heading,time,heading);
            drawnow limitrate

        record_orientation(k,:) = [time roll pitch heading];
        k = k+1;
    end

end
```

REFERENCES

[1] Kirk Hovell and Steve Ulrich. Experimental validation for tethered capture of spinning space debris. In *AIAA Guidance, Navigation, and Control Conference*, page 1049, 2017.

[2] Donald J Kessler and Burton G Cour-Palais. Collision frequency of artificial satellites: The creation of a debris belt. *Journal of Geophysical Research: Space Physics*, 83(A6):2637–2646, 1978.

[3] David Wright. The current space debris situation. In *Union of Concerned Scientists (UCS), Beijing Orbital Debris Mitigation Workshop*, 2010.